

On the Proper Estimation of the Confidence Interval for the Design Formula of Blast-Induced Vibrations with Site Records

W. M. Yan · Ka-Veng Yuen

Received: 3 August 2013 / Accepted: 15 February 2014 / Published online: 5 March 2014
© Springer-Verlag Wien 2014

Abstract Blast-induced ground vibration has received much engineering and public attention. The vibration is often represented by the peak particle velocity (PPV) and the empirical approach is employed to describe the relationship between the PPV and the scaled distance. Different statistical methods are often used to obtain the confidence level of the prediction. With a known scaled distance, the amount of explosives in a planned blast can then be determined by a blast engineer when the PPV limit and the confidence level of the vibration magnitude are specified. This paper shows that these current approaches do not incorporate the posterior uncertainty of the fitting coefficients. In order to resolve this problem, a Bayesian method is proposed to derive the site-specific fitting coefficients based on a small amount of data collected at an early stage of a blasting project. More importantly, uncertainty of both the fitting coefficients and the design formula can be quantified. Data collected from a site formation project in Hong Kong is used to illustrate the performance of the proposed method. It is shown that the proposed method resolves the underestimation problem in one of the conventional approaches. The proposed approach can be easily conducted using spreadsheet calculation without the need for any additional tools, so it will be particularly welcome by practicing engineers.

Keywords Bayesian analysis · Blasting · Explosions · Ground vibration · Monte Carlo simulation · Reliability · Scaled distance

Abbreviations

dof Degrees of freedom
PPV Peak particle velocity
SD Scaled distance

List of symbols

a, b Fitting coefficients of charge weight scaling laws
 c_0 Normalizing constant
 d Distance between the blasting source and the receiver
 D Database
 N Number of measurements in the dataset
 N_s Number of Monte Carlo samples
 v Peak particle velocity (PPV)
 $v_{84\%}, v_{95\%}$ 84 and 95 % confidence values of the PPV, respectively
 W Charge weight per delay
 Σ Covariance matrix
 χ Level of confidence
 ε Model output error
 ρ Correlation coefficient
 σ Standard deviation

Functions

E Expected value
 J_g Goodness-of-fit function
 p Probability density function
 $SE(y, x)$ Standard error of predicted y with varying x

W. M. Yan (✉)
Department of Civil Engineering, The University of Hong Kong,
Pokfulam, Hong Kong, China
e-mail: ryanyan@hku.hk

K.-V. Yuen
Department of Civil and Environmental Engineering, University
of Macau, Av. Padre Tomás Pereira, Taipa, Macau, China
e-mail: kvyuen@umac.mo

t	Student's t distribution
Var	Variance
Φ	Inverse of quantile function

Subscripts

i, j	Index
m	Measured value
α	Confidence level

Superscripts

\wedge	Optimal value
-	Mean

1 Introduction

Modern cities are usually congested and the supply of space becomes an emerging issue. The use of underground spaces, rock caverns, or partial removal of rocky hills becomes attractive to society. The drill-and-blast method is commonly adopted to break the rock mass, turn it into fragments of handleable size, and, therefore, to create spaces. Records showed that the discovery of explosives, also known as “gunpowder” or “black powder”, could be traced back to the 9th century in China (Needham 1987). Despite its long history, the well-documented use of explosives to replace mechanical digging in mining engineering can only be traced back to about 400 years ago (Persson et al. 1993). Nowadays, a wide variety of explosives having different compositions and performance characteristics are used for rock blasting, e.g., ammonium nitrate/fuel oil (ANFO), dynamite, emulsion, etc. With the advances in science and technology, the efficiency and safety of explosives no longer remains the sole concern. On the other hand, blast-induced vibrations and, thus, damage, particularly in densely populated urban areas, arouses more public attention. Excessive vibration does not only cause human annoyance but also leads to cracks or even the collapse of nearby structures. A huge amount of insurance claims could be a big concern.

In blast engineering practice, vibration is usually described simply by the peak particle velocity (PPV). Based on the consideration of energy decay, the empirical relationship among the PPV, the charge weight per delay, and the distance from the blast source to the receiver can be formulated. Engineers use the established relation to make a decision on the amount of explosives subject to a given PPV limit, which is often specified either by the client or governing bodies. In a blasting project, site-specific fitting coefficients would be preferable, as they include more precise site-specific geological and blasting information (such as rock quality, type of explosive, delay time, etc.). However, they can only be obtained in a progressive manner, since vibration records are

gradually collected at different stages of the project. How to use limited site-specific data to obtain reliable PPV prediction becomes a burning issue. In recent years, probabilistic analysis has aroused more and more attention in geotechnical engineering in order to deal with various types of modeling error and uncertainty (Griffiths and Fenton 1998; Zhang et al. 2004, 2009; Fenton and Griffiths 2005, 2008; Phoon and Kulhawy 2005; Yuen and Katafygiotis 2005; Griffiths et al. 2009; Huang et al. 2010; Ching et al. 2010, 2012; Phoon et al. 2010; Wang 2011; Wang et al. 2010; Yuen 2010a, b; Blair 2011a, b; Yuen and Mu 2011; Ching and Phoon 2012; Chiu et al. 2012a, b; Yan et al. 2012, 2013; Cao and Wang 2012, 2014; etc.). In this study, a methodology which employs the Bayesian probabilistic approach to shed light on the prediction of the PPV is presented.

The main objective of this paper is to demonstrate the process of deriving a probabilistic-based blast design formula using site-specific vibration records. A reliable confidence level of the PPV can be constructed by the proposed techniques with different computational efforts. It will be shown that a simple spreadsheet can be developed by the users to perform the calculation, without the need for any add-on tools. The proposed method is extremely useful and friendly to engineers to better predict the magnitude of blast-induced vibration when site-specific data are particularly limited at an early stage of a project.

2 Empirical Design Formula

Blair (2011a) has comprehensively reviewed two broad categories of vibration prediction methods being employed in blast engineering: the waveform superposition technique and the charge weight scaling technique, respectively. The study concluded that the charge weight scaling technique remains the most widely used approach to predict vibrations due to rock blasting. Over the past several decades, many different empirical formulas have been proposed to estimate the PPV from the amount of charge weight per delay W and the distance between the blasting source and the receiver d (Duvall and Petkof 1959; Langefors and Kihlström 1963; Davies et al. 1964; Ambraseys and Hendron 1968; Bureau of Indian Standards, BIS 1973; Ghosh and Daemen 1983; Pal Roy 1993). Nevertheless, basic flaws in the charge weight scaling laws have been discussed by Blair (2004) in detail. Among these formulas, two of them proposed by Duvall and Petkof (1959) and Ambraseys and Hendron (1968), respectively, are the most common ones. They are often referred to as the square- and cube-root attenuation formula, respectively. The functional forms of these formulas are obtained from the consideration of energy decay:

$$v = a_2(\text{SD}_2)^{-b_2} = a_2 \left(\frac{d}{\sqrt{W}} \right)^{-b_2} \tag{1}$$

$$v = a_3(\text{SD}_3)^{-b_3} = a_3 \left(\frac{d}{\sqrt{[3]W}} \right)^{-b_3} \tag{2}$$

where v is the PPV value in mm/s; d and W are the distance in m and charge weight per delay in kg; $\text{SD}_k = d/\sqrt{[k]W}$ ($k = 2, 3$) is called the scaled distance; and a_k and b_k ($k = 2, 3$) are two positive fitting constants calibrated from a given database of blast records. Traditionally, the cube-root scaling law is used for airblast and is rarely used to describe ground vibration. It is worth noting that the formulas are empirical. Therefore, the coefficient values cannot be derived in an analytical manner.

To estimate the regression coefficients, the vibration records of a project are collected and plotted in the $\ln v - \ln \text{SD}$ space. Data points are always scattering severely due to the fact that each blast is carried out under different conditions. In other words, there are other influencing factors not being incorporated into the formula. They include the difference in geology, the type of explosives, the geometry of the explosions, the blast timing, etc. A simple linear regression technique has been used to derive the “best-fitted” line for the collected data. Various statistical approaches can then be undertaken to derive the confidence level of the blast-induced vibration. By assuming a log-normal occurrence of the PPV at any particular scaled distance, Dowding (1985, 1996) presented an approximate statistical method to derive the 84 and 95 % confidence lines of the PPV using the standard error of the prediction (Benjamin and Cornell 1970). The 95 % confidence line refers to the PPV value that will not be exceeded in 95 out of 100 blasts. In other words, the 95 % confidence line can be viewed as the 95th percentile line. Equations (3a) and (3b) summarize the respective confidence lines:

$$v_{84\%} = 10^{\hat{v}(\hat{a}, \hat{b}; \text{SD}) + \text{SE}(\log(v), \log(\text{SD}))} \tag{3a}$$

$$v_{95\%} = 1.645 \times 10^{\hat{v}(\hat{a}, \hat{b}; \text{SD}) + \text{SE}(\log(v), \log(\text{SD}))} \tag{3b}$$

where $v_{84\%}$ and $v_{95\%}$ are the 84 and 95 % confidence lines, respectively; $\hat{v}(\hat{a}, \hat{b}; \text{SD})$ is the predicted v at SD based on the best-fitted parameters \hat{a} and \hat{b} derived from regression analysis; and $\text{SE}(\log(v), \log(\text{SD}))$ is the standard error of the predicted $\log(v)$, which is given by:

$$\begin{aligned} \text{SE}(\log(v), \log(\text{SD})) &= \text{SE}(Y, X) \\ &= \sqrt{\frac{1}{N-2} \left[\sum (Y - \bar{Y})^2 - \frac{[\sum (X - \bar{X})(Y - \bar{Y})]^2}{\sum (X - \bar{X})^2} \right]} \end{aligned} \tag{4}$$

in which $Y = \log(v)$ and $X = \log(\text{SD})$ for brevity, and N is the total number of datasets. This is referred to as Method I

in this investigation. It is worth noting that a set of commonly used empirical fitting coefficients in Hong Kong was derived based on this approach (Li and Ng 1992).

Statistically, a confidence interval for a new observation Y_α can be evaluated by the following equation (Draper and Smith 1981):

$$\begin{aligned} Y_\alpha &= \hat{Y} \pm t \left(0.5 + \frac{\alpha}{2}, \text{dof} \right) \times \text{SE}(Y, X) \\ &\times \sqrt{1 + \frac{1}{N} + \frac{(X - \bar{X})^2}{\sum (X - \bar{X})^2}} \end{aligned} \tag{5}$$

where Y and X is assumed to be linearly related; \hat{Y} is the prediction based on the best-fitted parameters resulting from linear regression analysis; α denotes the confidence interval, say 0.9; t represents the Student’s t distribution; dof denotes the degrees of freedom, which is $N - 2$ in this case; and $\text{SE}(Y, X)$ is the standard error of the prediction referring to Eq. (4). This is referred to as Method II in this study.

Finally, engineers can use the confidence line as a design curve to determine the appropriate amount of explosives for each blast operation, as illustrated in the following. A horizontal line at a prescribed PPV limit cuts the design curve at a scaled distance. This scaled distance can be used to calculate the charge weight per delay of the blasts when the distance between the blast source and the sensitive receiver is known. As a result, the amount of charge weight per delay can be determined.

Recently, Blair (2011a) presented a probabilistic analysis in which the probability of exceeding a prescribed PPV limit can be directly computed using a simple spreadsheet when the set of site-specific vibration data is given. The strength of this method is that only the recorded data are needed and the only assumption involved is that the scatter in data in forthcoming blast activities will be similar to that of the previously recorded blasts. The method offers a simple yet robust way to plan a blast.

3 Blasting Projects and Vibration Limits in Hong Kong

In Hong Kong, the use of explosives is controlled by the Hong Kong Ordinance Chapter 295: Dangerous Goods Ordinance. The regulations are monitored and controlled by the Mines Division of the Civil Engineering and Development Department (CEDD). A blasting assessment report should be prepared in accordance to the guidelines/requirements given by the Geotechnical Engineering Office (GEO 2006) and Buildings Department (2007). Various guidelines have been provided in Hong Kong when blasting is adopted for site formation/foundation works (Wong and Pang 1992; Buildings Department 2004, 2007, 2009; Hong Kong Special Administrative Region, HKSAR 2006;

etc.). In general, a prescribed PPV limit of 25 mm/s is adopted regardless of the vibration frequency. However, this limit could become more stringent when other stakeholders are involved. For instance, the PPV limit for water-retaining structures, electric power stations, and historical monuments could drop to 13, 11, and 5 mm/s, respectively, as specified by different parties. Furthermore, a no-blast zone can be set up depending on the nature of the sensitive receivers. For example, blasting is generally not permitted to be carried out within 3 m of a tunnel owned by the Mass Transit Railway Corporation Limited or within the protective zones of the Water Supplies Department unless prior approval is obtained.

In recent years, there has been a sharp increase in the number of infrastructure projects in Hong Kong. These projects can be broadly divided into three main categories according to their functions: (1) transportation systems, mainly due to the extension lines of the underground transits and some other road tunnels; (2) drainage systems, which were designed to relieve the flooding risk of some low-lying urban areas in Hong Kong; and (3) site formation, the restoration of quarry or hilly terrain for land development. Furthermore, the HKSAR Government has been promoting the development of rock caverns as an option with great potential to increase the land supply in Hong Kong, whereas other options like reclamation, redevelopment, and land rezoning and resumption are more controversial and difficult to be implemented. Therefore, increasing rock drill-and-blast activities have taken place in the past few years and this trend is expected to continue in the coming years or even decades. In Hong Kong, at the early stage of a blasting project when insufficient field monitoring records are available to establish a more precise site-specific fitting formula, the fitting coefficients (and, thus, formula) suggested by Li and Ng (1992) are often referred. Li and Ng (1992) summarized 520 sets of blasting data which were collected between 1984 and 1991. The database contained blast records taken from various types of projects, including site formation, quarrying, tunneling, caisson sinking, excavation, and submarine blasting. Blasting can be categorized into confined and free-face blasts. Confined blasting includes most of the tunnel blasts and sink blasts, while free-face blasting includes site formation and excavation.

Linear regression analysis of the records was undertaken to determine the best-fitted coefficients a_2 and b_2 in Eq. (1) and, thus, the best-fitted line. As mentioned in the previous section, Li and Ng (1992) then constructed the 84 and 95 % confidence lines following the method suggested by Dowding (1996), as shown in Eqs. (3a) and (3b). Table 1 summarizes the fitting constants from their study. Before sufficient site-specific vibration records are available, the Hong Kong Government accepts the 84 % confidence line

Table 1 Fitting coefficients suggested by Li and Ng (1992)

Description	a_2	b_2
Best-fitted line	310	1.22
84 % Confidence level line	644	1.22
95 % Confidence level line	1,032	1.22

as proposed by Li and Ng (1992) to be adopted in the blast design of a different project. As presented earlier, the amount of explosive charge per delay can then be determined based on the known physical distance between the blast source and the receiver, and the prescribed PPV limit.

Nevertheless, the use of the fitting coefficients provided by Li and Ng (1992) in a different project is definitely not ideal. The coefficients simply miss out any site-specific characteristics of the project, such as the geological setting and material properties. It is, therefore, highly desirable to obtain site-specific fitting coefficients and, thus, to use the design formula containing these coefficients for subsequent blasting activities. However, site-specific measurements can only be obtained in a progressive manner. The reliability of a PPV-scaled distance relation often becomes questionable when very few data are used to calibrate the fitting coefficients. In Hong Kong, the number of minimum blast records required to derive the site-specific fitting constants is advised by the Mines Division on a case-by-case basis.

More importantly, the modeling uncertainty is not explicitly taken into account in the construction of the confidence line in either Methods I or II. The modeling uncertainty becomes more critical when site-specific fitting coefficients are derived at the early stage of a project where only very limited monitored data are available. In this case, the uncertainty of the model parameters, and, hence, the model output, is so large such that negligence of the modeling uncertainty induces substantial error in establishing the confidence interval. A Bayesian probabilistic method is presented in this study to resolve this problem. Details of the method are presented next.

4 Bayesian Framework

Consider a database D with N blast records that comprise the measurements of v , d , and W . The scaled distance SD_2 can then be computed from d and W . With the Bayesian probabilistic approach, the following objectives can be achieved: (a) to estimate the optimal model parameters a_2 and b_2 in the empirical relation; (b) to quantify their associated uncertainty by evaluating their posterior distribution; and (c) to quantify the uncertainty of the empirical formula output for the construction of the confidence interval of any prescribed reliability levels.

The square-root formula shown in Eq. (1) is used here to illustrate the computational concept of the proposed method. It should be noted that the same procedure is also valid for Eq. (2) when airblast is concerned. First, Eq. (1) is rewritten as a linear regression problem:

$$\ln v_m = \ln v + \varepsilon = \ln a_2 - b_2 \ln SD_2 + \varepsilon \tag{6}$$

where v_m is the measured PPV value and ε represents the model output error in the logarithmic scale. In the $\ln v - \ln SD_2$ space, the term $\ln a_2$ represents the vertical intercept of the fitting line at $SD_2 = 1$, while $-b_2$ gives its slope. The model output error, which is a collective quantity of the measurement noise and the modeling error, is assumed to be Gaussian with zero mean and variance σ_ε^2 . In this case, the modeling error includes the deficiency of this simple empirical formula in considering the underlying problem. This includes the negligence of the characteristics of wave-transmitting media, the geometric setting of the blast area, the blast-hole configurations, the type of explosives, etc. The variable σ_ε^2 represents the variance of the model output error and it is an unknown parameter to be estimated using the measurements. The updated/posterior probability density function (PDF) of the model parameters given database D can be expressed as (Yan et al. 2009):

$$p(\ln a_2, b_2, \sigma_\varepsilon | D) = c_0 p(\ln a_2, b_2, \sigma_\varepsilon) (2\pi)^{-N/2} \sigma_\varepsilon^{-N} \times \exp \left[-\frac{N}{2\sigma_\varepsilon^2} J_g(\ln a_2, b_2 | D) \right] \tag{7}$$

where c_0 is the normalizing constant such that the volume under the updated PDF is unity and $p(\ln a_2, b_2, \sigma_\varepsilon)$ is the prior PDF of the uncertain parameters to express the user’s judgment about the relative plausibility of the values of these parameters before the data are obtained. In this study, a non-informative prior distribution is employed so that the prior PDF can be absorbed into the normalizing constant. As a result, the Bayesian inference will rely solely on the likelihood of the measurements. The function $J_g(\ln a_2, b_2 | D)$ is the goodness-of-fit function which indicates how well the model fits the data (Yuen and Kuok 2011) and it takes the following form:

$$J_g(\ln a_2, b_2 | D) = \frac{1}{N} \sum_{i=1}^N [\ln v(a_2, b_2; SD_{2(i)}) - \ln v_{m(i)}]^2 \tag{8}$$

where $v(a_2, b_2; SD_{2(i)})$ is the model output of the i th record with parameters $\ln a_2$ and b_2 , and $v_{m(i)}$ is the corresponding measured value. This function gives the variance of the fitting error between the measurements and the corresponding model outputs. The optimal model parameters $\ln \hat{a}_2$ and \hat{b}_2 can be obtained by maximizing the updated PDF $p(\ln a_2, b_2, \sigma_\varepsilon | D)$ in Eq. (7) (the symbol \hat{x} is used to denote the optimal value of the variable x).

There are three unknowns ($\ln a_2$, b_2 , and σ_ε^2) for the empirical model considered in Eq. (1). Nevertheless, with a non-informative prior distribution, the optimization problem can be decomposed into two sub-problems: (i) to minimize the objective function J_g with respect to the model parameters $\ln a_2$ and b_2 , and (ii) to maximize the updated PDF in Eq. (7) with respect to σ_ε^2 given the model parameters from step (i). The first optimization problem can be tackled by solving simultaneously $\partial J_g / \partial \ln a_2 = 0$ and $\partial J_g / \partial b_2 = 0$, and this yields the following closed-form solution of the optimal parameters (Yuen 2010a):

$$\begin{bmatrix} \ln \hat{a}_2 \\ \hat{b}_2 \end{bmatrix} = \begin{bmatrix} N & -\sum_{i=1}^N \ln SD_{2(i)} \\ -\sum_{i=1}^N \ln SD_{2(i)} & \sum_{i=1}^N [\ln SD_{2(i)}]^2 \end{bmatrix}^{-1} \times \begin{bmatrix} \sum_{i=1}^N \ln v_{m(i)} \\ -\sum_{i=1}^N \ln SD_{2(i)} \ln v_{m(i)} \end{bmatrix} \tag{9}$$

After obtaining the optimal model parameters $\ln \hat{a}_2$ and \hat{b}_2 , the fitting error variance $\hat{\sigma}_\varepsilon^2$ can be found by solving $\partial p(\ln a_2, b_2 | D) / \partial \sigma_\varepsilon = 0$. By Beck and Katafygiotis (1998), it is equal to the minimum of the goodness-of-fit function:

$$\hat{\sigma}_\varepsilon^2 = \min_{\ln a_2, b_2} J_g(\ln a_2, b_2 | D) = J_g(\ln \hat{a}_2, \hat{b}_2 | D) \tag{10}$$

Furthermore, the posterior covariance matrix $\Sigma_{\ln a_2, b_2}$ for the model parameters can be computed as follows (Yuen 2010a):

$$\Sigma_{\ln a_2, b_2} = \hat{\sigma}_\varepsilon^2 \begin{bmatrix} N & -\sum_{i=1}^N \ln SD_{2(i)} \\ -\sum_{i=1}^N \ln SD_{2(i)} & \sum_{i=1}^N [\ln SD_{2(i)}]^2 \end{bmatrix}^{-1} \tag{11}$$

This allows for the computation of not only the posterior variance of $\ln a_2$ and b_2 , but also the correlation coefficient between them. In the following sections, two different approaches, Monte Carlo simulation and direct computation, respectively, involving different degrees of computational effort, to derive the confidence intervals of the vibration formula will be presented.

5 Reliability Analysis

5.1 Monte Carlo Simulation

Instead of obtaining a single empirical relationship using the optimal values for $\ln a_2$ and b_2 , the posterior PDF $p(\ln a_2, b_2, \sigma_\varepsilon | D)$ in Eq. (7) is used to generate numeric

samples of the parameters for the quantification of the modeling uncertainty. Specifically, a large number of samples N_s of these parameters ($\ln a_{2(j)}$, $b_{2(j)}$, $\sigma_{\varepsilon(j)}$; $j = 1, 2, \dots, N_s$) can be simulated efficiently by the Markov chain Monte Carlo simulation (Metropolis et al. 1953; Hastings 1970). Then, the j th PPV sample can be estimated by Eq. (6), as shown below:

$$\ln v_{(j)} = \ln a_{2(j)} - b_{2(j)} \ln SD_2 + \varepsilon_{(j)} \tag{12}$$

where the measurement noise $\varepsilon_{(j)}$ can be generated by the Gaussian generator with zero mean and variance $\hat{\sigma}_{\varepsilon(j)}^2$. By doing so, a large collection of N_s PPV samples at any values of scaled distance can be generated. Then, at any particular scaled distance, the PPV values are sorted to identify the corresponding value at a prescribed percentile level. For example, the 5th and 95th percentile levels are used in this study. Therefore, the lower and upper bounds of the PPV for the desired confidence levels can be obtained under such a scaled distance (e.g., the 5th and 95th percentiles give a 90 % confidence interval). These steps are repeated for different scaled distances and, thus, a confidence region for different scaled distance values can be obtained. It is referred to as Method III in this study.

5.2 Direct Computation

Alternatively, a direct approach can be used with less computation. First, Eq. (6) can be rewritten as follows:

$$\ln v_m = [1 \quad -\ln SD_2] \begin{bmatrix} \ln a_2 \\ b_2 \end{bmatrix} + \hat{\sigma}_{\varepsilon} \bar{\varepsilon} = \mathbf{X}^T \mathbf{C} + \hat{\sigma}_{\varepsilon} \bar{\varepsilon} \tag{13}$$

where $\mathbf{X} = [1 \quad -\ln SD_2]^T$, $\mathbf{C} = [\ln a_2 \quad b_2]^T$, and $\bar{\varepsilon}$ follows the standard Gaussian distribution (denoted by $N(0, 1)$). The variance of ε is taken as the optimal value $\hat{\sigma}_{\varepsilon}^2$ in Eq. (10) to simplify the calculation. The variance of the first term on the right-hand side of Eq. (13) can be written as:

$$\text{Var}(\ln v) = \mathbf{X}^T \mathbf{E} \left[(\mathbf{C} - \hat{\mathbf{C}}) (\mathbf{C} - \hat{\mathbf{C}})^T \right] \mathbf{X} \tag{14}$$

where $\hat{\mathbf{C}}$ is the optimal parameter vector. By definition, the term $\mathbf{E}[(\mathbf{C} - \hat{\mathbf{C}})(\mathbf{C} - \hat{\mathbf{C}})^T]$ is the posterior covariance matrix $\Sigma_{\ln a_2, b_2}$ as shown in Eq. (11) (Yuen 2010a). Therefore, the variance of $\ln v_m$ can be evaluated as follows.

$$\text{Var}(\ln v_m) = \mathbf{X}^T \Sigma_{\ln a_2, b_2} \mathbf{X} + \hat{\sigma}_{\varepsilon}^2 \tag{15}$$

Therefore, it can be seen clearly that the confidence interval bounds are in general parabolic curves instead of straight lines.

The standard deviation $\sigma_{\ln v_m}$ of $\ln v_m$ can then be quantified (i.e., $\sigma_{\ln v_m} = \sqrt{\text{Var}(\ln v_m)}$). The upper and lower bounds of $\ln v_m$ ($\ln v^{\pm}$) with various degrees of confidence levels can be formulated by:

$$\ln v^{\pm} = \ln v(\ln \hat{a}_2, \hat{b}_2) \pm \chi \sigma_{\ln v_m} \tag{16}$$

where χ is associated with the confidence level specified by the user. For a confidence level of α , it is given by $\chi = \Phi^{-1}(0.5 + \alpha/2)$, where Φ^{-1} is the quantile function [i.e., the inverse function of the cumulative distribution function (CDF) of the standard Gaussian random variable]. For instance, $\chi = 1.645$ and 1.96 give curves enclosing 90 and 95 % of the probability for the prediction of $\ln v_m$, respectively. This is referred to as Method IV. Both Methods III and IV originate from the same Bayesian approach, but Method IV is much simpler than Method III (Monte Carlo simulation), as less computational effort is required. It is favorable to practicing engineers in comparison with Method III since the analysis can be done simply by a standard package of spreadsheets without the need for any add-on tools. The ‘‘Appendix’’ shows the template of such a spreadsheet for readers’ reference. Detailed steps of the procedure are also given.

6 Case Study

Blast-induced vibration data collected from a site formation project in Hong Kong are used to demonstrate the performance of the proposed methods. The project comprises the formation of a ~20-ha platform and the construction of infrastructure facilities, including roads, bridges, retaining structures, and drainage works for residential and community uses. The site is a rocky rugged area developed on granite. The site works commenced on Jan 31, 2008 and the tasks are expected to be completed between 2011 and 2014 in stages. A large amount of rock blast activities have been carried out in the three major blasting zones inside the site. Both cartridge and bulk emulsion are used as explosives and the blasts are initiated by the Austin non-electric detonator. A total of 194 sensitive receivers have been identified in the vicinity of the site, including high-rise residential blocks, slopes, roads, schools, transformer room, water reservoir, etc.

Ground vibration is monitored using a NOMIS 7000 seismograph. The sensor is able to record vibration in the range 0.127 and 254 mm/s (0.005 and 10 in/s). The vibration data recorded on slopes (identified as one of the sensitive receivers) are used for the analyses presented in this paper. Note that the same procedure is applicable to other sensitive receivers. In a blast record, the maximum vibration among the vibrations in three orthogonal

Table 2 Summary of data records

Data collection: from May 11, 2008 to:	Number of data (N_1)	Range [minimum, maximum]			
		PPV (mm/s)	Charge weight per delay, W (kg)	Distance, d (m)	Scaled distance, SD_2 (m/ $\sqrt{\text{kg}}$)
Dec 30, 2008	40 ^a	[1.27, 30.1]	[4, 23]	[43.1, 248.8]	[15.3, 57.1]
Feb 27, 2009	82 ^a	[1.1, 30.1]	[3, 23]	[43.1, 257.3]	[15.3, 72.2]
Mar 30, 2009	119 ^a	[1.1, 30.1]	[1.4, 23]	[43.1, 257.3]	[15.3, 105.7]
Apr 30, 2009	153 ^a	[1.1, 30.1]	[1.4, 23]	[43.1, 257.3]	[15.3, 105.7]
Jul 31, 2009	196 ^a	[1.1, 30.1]	[1.4, 23]	[43.1, 376.2]	[15.3, 146.5]
Feb 28, 2011	957	[0.5, 33.4]	[1.1, 33.2]	[23.9, 376.2]	[10.0, 183.9]

^a Bayesian analysis is carried out on this database to derive the PDF of the fitting coefficients ($\ln a_2$ and b_2) and the fitting error variance σ_ε^2 . Confidence intervals will then be derived

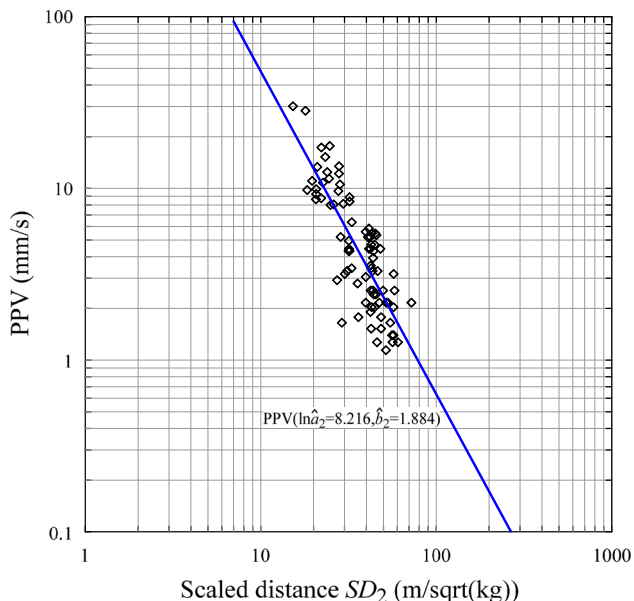


Fig. 1 Vibration data collected at the site ($N_1 = 82$)

directions is used as the PPV in the analysis. A total of 957 vibration records of bench blasting using cartridge emulsion were collected for blasts that had taken place from November 2008 to February 2011. In this study, the records are first separated into two groups. The first group contains only the blast records collected at the early stage of the project (N_1 data points), while the second group contains the remaining records (N_2 data points). As a result, $N_1 + N_2 = 957$. Later in this paper, the effect of N_1 on the prediction of vibration will be examined.

The records in the first group are used to estimate the fitting coefficients of the empirical formula and, thus, to provide an estimation of the PPV with the scaled distance according to the methods shown in Eqs. (3a), (3b), and (5), Methods I and II, respectively. Furthermore, the same N_1 data points are fed into the proposed Bayesian methods and the confidence interval can be constructed based on the aforementioned reliability analyses. The effect of N_1 on the prediction performance of the formula can be studied. The entire database (957 data) is then used to assess the

prediction performance of these approaches. Table 2 summarizes the number of blast records and ranges of parameters at different stages of the project. It is noted that the database for $N_1 = 119$ and $N_1 = 153$ contain the same ranges of PPV, W , d , and SD_2 . However, the data distributions are slightly different, as the latter contains more data points. The analyses will be carried out for the cases of $N_1 = 40, 82, 119, 153,$ and 196 , corresponding to the first few stages of the project.

7 Results

7.1 Fitting Coefficients for $N_1 = 82$

In this section, the results obtained by analyzing the database with $N_1 = 82$ (records collected up to Feb 27, 2009; 3 months of blasting) are used to demonstrate the proposed Bayesian methods. Note that similar analyses are performed also for other values of N_1 , namely, 40, 119, 153, and 196 (see Table 2) to investigate the effect of N_1 and the results will be shown in a later section. Figure 1 shows the 82 PPV records plotted against the corresponding scaled distance. Figure 2 shows the conditional posterior PDF $p(\ln a_2, b_2 | D, \hat{\sigma}_\varepsilon)$ computed using Eq. (7) and its contours. The optimal coefficients are found to be $\ln \hat{a}_2 = 8.216$ and $\hat{b}_2 = 1.884$ (for $N_1 = 82$), at which the goodness-of-fit function $J_g(\ln a_2, b_2 | D)$ is minimized. The solid line shown in Fig. 1 represents this “best-fitted” line which is associated with the optimal coefficients. Table 3 summarizes the optimal values ($\hat{\cdot}$), and covariance (σ^2) of the estimated parameters $\ln a_2, b_2,$ and ε for different N_1 . Furthermore, the column $\rho(\ln a_2, b_2)$ shows the correlation coefficients between $\ln a_2$ and b_2 for different cases. One can see that the two model parameters are highly correlated ($\rho > 0.99$).

7.2 Confidence Interval for $N_1 = 82$

The confidence line (CL) or confidence interval (CI) is constructed by the four different approaches previously mentioned: (Method I) approximate method by Dowding

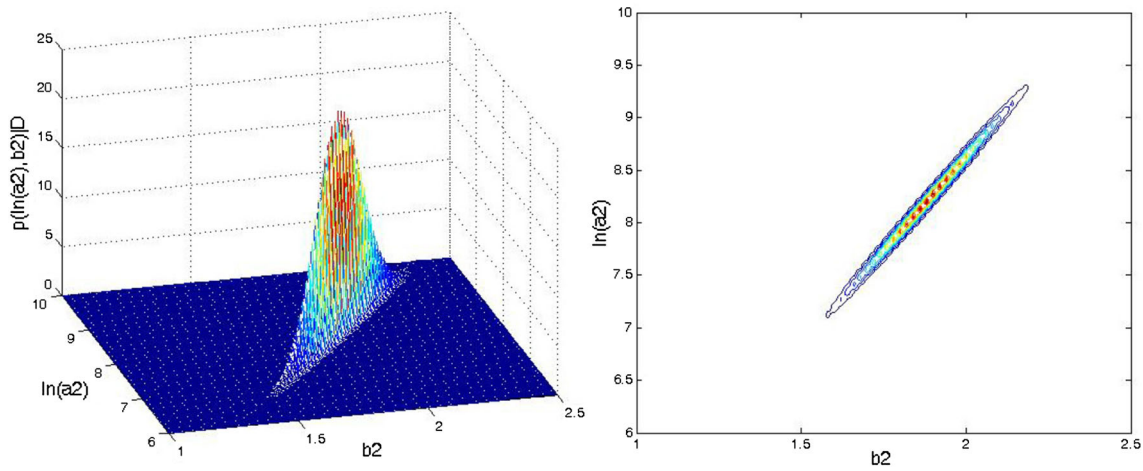


Fig. 2 Posterior probability density function (PDF) of $\ln a_2$ and b_2 ($N_1 = 82$)

Table 3 Statistics of the obtained fitting coefficients for different N_1

N_1	$\ln \hat{a}_2$	$\sigma_{\ln a_2}^2$	\hat{b}_2	$\sigma_{b_2}^2$	$\sigma(\ln a_2, b_2)$	$\rho(\ln a_2, b_2)$	$\hat{\sigma}_\varepsilon^2$
40	8.3581	0.3824	1.9630	0.0300	0.1066	0.9951	0.1486
82	8.2157	0.2667	1.8840	0.2021	0.0738	0.9956	0.1940
119	8.0229	0.1963	1.8167	0.0147	0.0534	0.9956	0.2039
153	7.7790	0.1648	1.7332	0.0122	0.0447	0.9956	0.2215
196	7.4509	0.0991	1.6361	0.0072	0.0265	0.9944	0.2178

(1996) [see Eqs. (3a) and (3b)], which derives CL; (Method II) statistical approach shown in Eq. (5), which gives CI; (Method III) Monte Carlo simulation for CI; and (Method IV) direct computation for the CI. Details of each method are shown as follows.

In Method I, the best-fitted line is first obtained by linear regression analysis with N_1 data points (82 in this case, represented by diamonds in Fig. 3). It gives $a_2 = 3699$, $b_2 = 1.884$, and $R^2 = 0.677$. The 95 % CL, which is represented by the dotted line in Fig. 3, is then constructed using Eq. (3b). All 957 blast data points (denoted by the triangles) are then plotted in the same figure. Except for two data points, they appear to show a minimum PPV of about 1.1 mm/s (1.143 mm/s by reading from the monitoring records). This is actually not the minimum detectable vibration as specified by the sensor, which is 0.127 mm/s, as mentioned earlier. The vibration magnitude of 1.143 mm/s is simply the maximum among the vibrations in three orthogonal directions recorded in the studied slopes, and this maximum is adopted for the analysis. When other sensitive receivers are studied (for instance, transformer rooms), smaller maximum PPV (<1.1 mm/s) can be found. However, the reason why many blasts tend to give a maximum PPV of about 1.1 mm/s on the studied slopes in an individual blast remains unclear. The performance of Method I is evaluated when the dotted line in

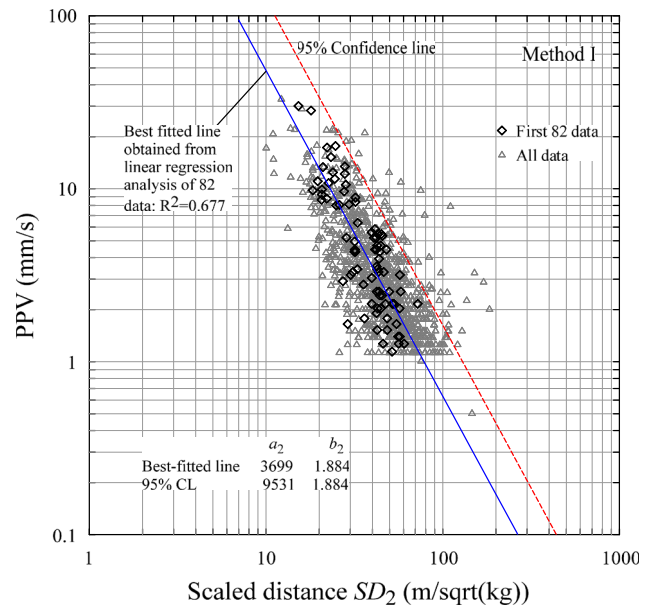


Fig. 3 Vibration data collected at the site. The best-fitted line (solid line) is obtained by linear regression, whereas the 95 % confidence line (dotted line) is derived according to Eq. (3b) (Method I)

Fig. 3 is compared to all the collected data. Among the total of 957 records, it is found that 51 points fall above this 95 % CL. It may give an impression that the result is,

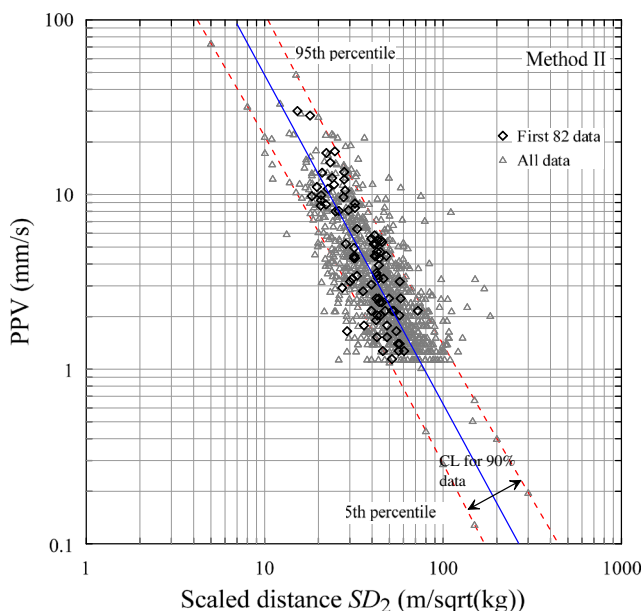


Fig. 4 Vibration data collected at the site. The dotted lines represent the 90 % confidence interval evaluated by Eq. (5) based on the first 82 data records (Method II)

indeed, very good ($51/957 = 5.3 \% = 5 \%$) and Method I performs well. This issue will be revisited later when the results from all four methods of analysis with different N_1 are ready.

The performance of Method II is then investigated. Figure 4 shows the best fitted line (solid line) and the 5th and 95th percentile lines (dotted lines), which offer a 90 % confidence interval, derived according to Eq. (5) based on $N_1 = 82$. It is found that 81 ($81/957 = 8.5 \%$) and 87 (9.1 %) data points, among the 957 data records, fall below and above the two percentile lines, respectively.

Next, the results obtained using the proposed Monte Carlo approach is presented. First, note that the best-fitted line of the proposed approach is identical to conventional linear regression and the difference is in the confidence interval. According to the posterior PDF of the model parameters obtained from the Bayesian analysis, Markov chain Monte Carlo simulation is carried out to generate 500,000 samples of the uncertain parameters ($N_s = 500,000$). In other words, 500,000 sets of $\ln a_2$, b_2 , and ε can be obtained. For any scaled distance value, the corresponding values of $\ln v$ (and, thus, PPV) can be computed by using Eq. (12). In other words, 500,000 samples of the PPV value are obtained for any particular scaled distance value. The PPV values are then sorted to determine the percentile positions (i.e., the PPV values for the 5th and 95th percentiles in this application). Finally, by drawing

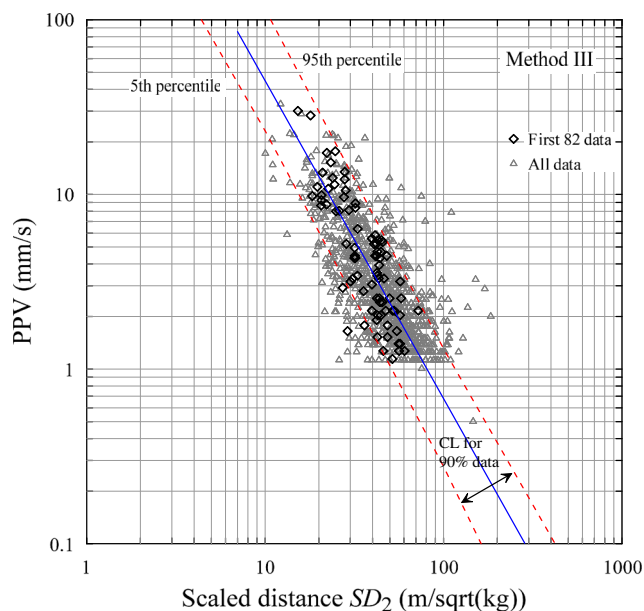


Fig. 5 Vibration data collected at the site. The dotted lines represent bound curves enclosing 90 % of the data from the Monte Carlo simulation ($N_s = 500,000$) based on the first 82 data records (Method III)

the two curves to connect these percentile positions at different scaled distances, the confidence interval can be obtained. In this problem, it is found that the bounds of the CI are slightly curved in the $\ln v - \ln SD_2$ space, and they are depicted in Fig. 5. The solid line represents the 50th percentile line of the 500,000 simulated PPV values, while the dotted lines (5th and 95th percentiles, respectively) enclose 90 % of the simulated vibration records. It is found that 83 and 96 records (i.e., 8.6 % and 9.8 % of the total of 957 records) fall below and above the 5th and 95th percentile lines, respectively.

Lastly, results of the direct computation method are presented. Equation (15) is used to quantify the variance of $\ln v_m$, which is summarized in Table 4. The term $\mathbf{X}^T \Sigma_{\ln a_2, b_2} \mathbf{X}$, which quantifies the uncertainty of the model parameters, decreases with increasing N_1 at any scaled distance. It is expected because the uncertainty of the model parameters should decrease when more data are collected for the analysis. As shown in the table, $\sigma_{\ln v_m}^2$ decreases noticeably with increasing N_1 at extreme SD_2 ($SD_2 = 1$ or $1000 \text{ m}/\sqrt{\text{kg}}$). At intermediate values of SD_2 , the change of $\sigma_{\ln v_m}^2$ with N_1 is minor. In fact, most of the collected data fall into the range $10 \leq SD_2 \leq 100 \text{ m}/\sqrt{\text{kg}}$. With a choice of $\chi = 1.645$, the 5th and 95th percentiles of $\ln v_m$ (i.e., enclosing 90 % of the data) can be computed. It is worth noting that a different choice of χ will give bounds

Table 4 Variance of the peak particle velocity (PPV) derived from different N_1 records

N_1	$\hat{\sigma}_e^2$	$\mathbf{X}\Sigma_{\ln a_2, b_2}\mathbf{X}^T$ and $(\sigma_{\ln v_m}^2)$			
		$SD_2 = 1$	$SD_2 = 10$	$SD_2 = 100$	$SD_2 = 1000$
40	0.1486	0.3824 (0.5310)	0.0506 (0.1992)	0.0369 (0.1855)	0.3414 (0.4900)
82	0.1940	0.2667 (0.4607)	0.0361 (0.2301)	0.0239 (0.2179)	0.2301 (0.4240)
119	0.2039	0.1952 (0.3991)	0.0275 (0.2313)	0.0159 (0.2197)	0.1605 (0.3644)
153	0.2215	0.1648 (0.3863)	0.0237 (0.2453)	0.0125 (0.2340)	0.1311 (0.3526)
196	0.2178	0.0991 (0.3169)	0.0151 (0.2329)	0.0070 (0.2248)	0.0748 (0.2926)

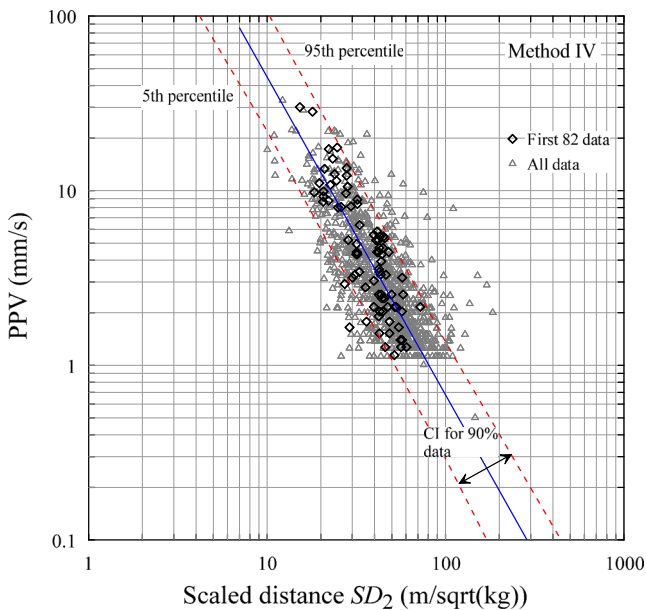


Fig. 6 Vibration data collected at the site. The dotted lines represent bound curves enclosing 90 % of the data from direct computation based on the first 82 data records (Method IV)

with different confidence intervals. Figure 6 shows the results of direct computation. The obtained percentile lines locate in essentially the same position as those derived from the Monte Carlo simulation. The results should be expected, as the two methods are essentially equivalent. It is found that 8.6 and 9.7 % of the data lie below and above the 5th and 95th percentile lines, respectively, when all blast records are used to quantify the performance of this direct computation method. The “Appendix” illustrates how a spreadsheet can be developed to carry out the study easily.

7.3 Effect of the N_1 Value

It is expected that the reliability of the confidence interval can be enhanced by using more data points for the Bayesian analysis to update the posterior PDF of the fitting coefficients. This is because more information about the

model can be reflected by a larger number of data points N_1 . The effect of N_1 on the reliability of the model prediction is studied and summarized as follows. As shown in Table 3, the number of data points, N_1 , used to evaluate the confidence intervals varies from 40 to 196, corresponding to about 4 to 20 % of the entire dataset. Note that, in a real project, the data are collected in a progressive manner. Increasing N_1 results in the reduction of the standard deviation of both fitting parameters ($\ln a_2$ and b_2). The trend is expected, as more measurements in a database give more information about the model and can, thus, reduce the uncertainty of the model prediction. Table 5 summarizes the effect of N_1 on the performance of the reliability of CL or CI. Method III (Monte Carlo simulation) and Method IV (direct computation) give essentially the same results. For brevity, only the results of Method IV are shown in the table. The following observations can be made:

1. At $N_1 = 40$, all methods give rather poor predictions. Yet, Method I, among all, appears to give the best performance: 10.9 % PPV of the 957 blasts fall above the 95 % CL, in comparison with 18.4 and 19.9 % for Methods II and IV, respectively.
2. By increasing N_1 , all methods show a decreasing amount of PPV falling above the 95 % CL and the 95th percentile line. In particular, Method I shows only 2.4 % of data lying above the 95 % CL when N_1 becomes 196, in comparison with 10.9 % at $N_1 = 40$.
3. Methods II and IV give very similar results, particularly when N_1 becomes large. The amount of data lying above the 95th percentile line decreases from about 19 to 5 % when N_1 increases from 40 to 196.

7.4 Performance of Various Methods

As shown in Table 5, it can be seen that there are always more than 5 % PPV measurements falling below the 5th percentile of both Methods II and IV. The number has an increasing trend with N_1 . It is due to the fact that more conservative blast design is made occasionally in a blasting

Table 5 Effect of N_1 on prediction reliability

N_1	Method I	Method II	Method IV ^a		
	Number of data falling above 95 % CL	Number of data falling below 5th percentile line	Number of data falling above 95th percentile line	Number of data falling below 5th percentile line	Number of data falling above 95th percentile line
40	104 (10.9 %)	66 (6.9 %)	176 (18.4 %)	74 (7.7 %)	190 (19.9 %)
82	51 (5.3 %)	81 (8.5 %)	87 (9.1 %)	82 (8.6 %)	93 (9.7 %)
119	38 (4.0 %)	88 (9.2 %)	64 (6.7 %)	90 (9.4 %)	70 (7.3 %)
153	28 (2.9 %)	93 (9.7 %)	50 (5.2 %)	94 (9.8 %)	51 (5.3 %)
196	23 (2.4 %)	97 (10.1 %)	45 (4.7 %)	97 (10.1 %)	45 (4.7 %)

^a The results obtained from Methods III and IV are very close. Therefore, only the results obtained from Method IV are shown in the table for brevity

project, where less explosive is used in some planned blasts. As a result, only small vibration is then recorded in some blasts, which explains the data scattering below the 5th percentile line. In practice, engineers are more concerned with the amount of vibration records which show the PPV exceeding the design limit, rather than those falling below a certain percentile line. When one examines the amount of PPV records lying above the 95 % CL or 95th percentile line predicted by $N_1 = 82$, Method I gives a close to 5 % prediction, which appears to outperform the other methods. However, it does not imply that Method I is a robust approach. The overconservatism of this method can be readily seen when N_1 increases (less than 3 % of data falling above the 95 % CL at $N_1 = 153$ and 196). An increase in N_1 , yet, does not improve the performance of this method. In other words, the method cannot learn from additional data. On the contrary, Methods II and IV (including Method III) show a clear improvement when an increasing amount of data are used to compute the prediction (i.e., close to 5 % of data is predicted to fall above the 95th percentile line with increasing N_1). Despite the fact that Method II gives very similar results to Method IV, the Bayesian-based Method IV is recommended. This is because, in this newly proposed method, the contribution of uncertainty from fitting parameters and modeling error can be clearly quantified, which offers better understanding of the model prediction.

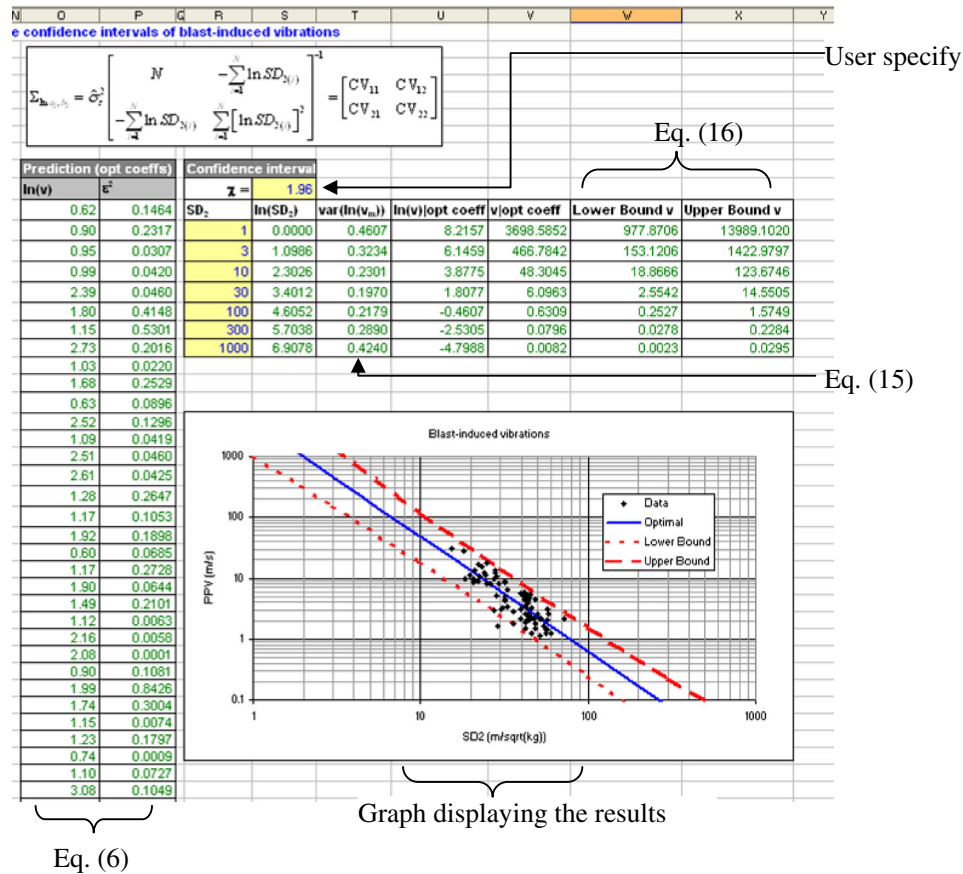
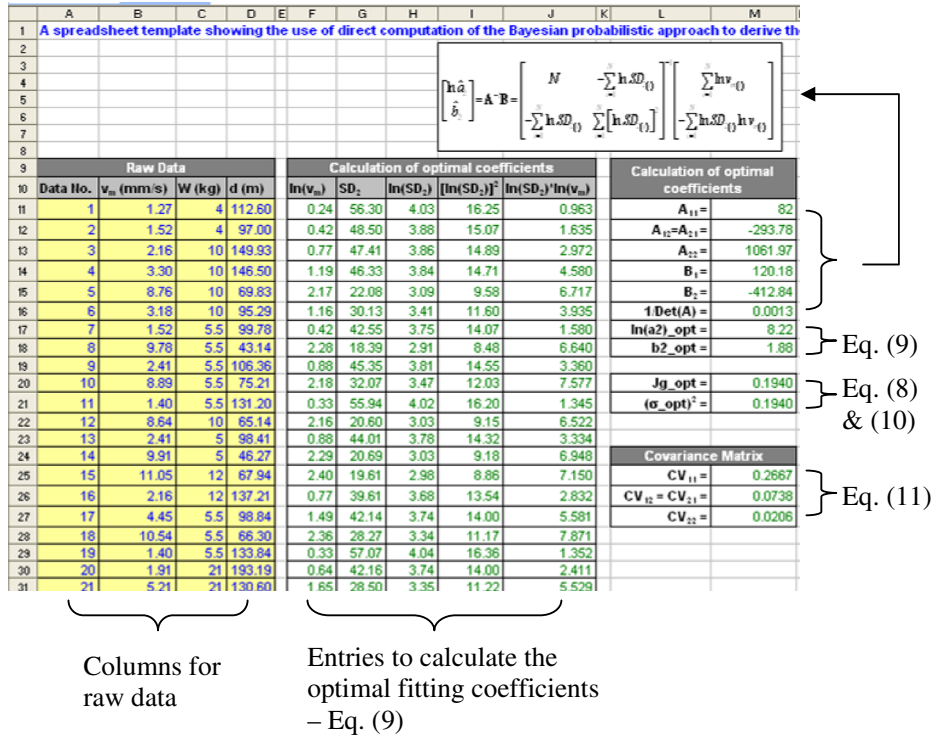
8 Conclusion

Blast-induced vibration has received much attention over the last several decades. Determination of the

explosive charge weight subject to a prescribed vibration limit is an important task. In this paper, two existing methods for the construction of confidence intervals of the blast design formula are reviewed. The problem is then revisited from a Bayesian probabilistic perspective, where uncertainty of the formula output can be explicitly quantified. By using the proposed methods, blast design formula with different confidence intervals can be obtained. Detailed computation of the methods and their performance are illustrated by a recent site formation project in Hong Kong where many rock blasting activities have been undertaken. First, both proposed methods are useful at the early stages of a blasting project when only limited site-specific data are available. They provide reliable confidence intervals of blast-induced vibrations and their results are essentially the same. Furthermore, the direct computation approach is extremely useful, as simple spreadsheet calculation can be developed by the users to conduct the analysis. Neither add-on tools nor complicated iterations are required for the analysis, and this would be very favorable to practicing engineers.

Acknowledgments The authors wish to acknowledge the support by grant nos. 201011159079 and HKU7171/10E provided by the University of Hong Kong and the Research Grants Council of Hong Kong, respectively. The authors would also like to thank the Special Duties (Works) Division of the Civil Engineering and Development Department and Ove Arup and Partners for providing the blasting data used in the study. The views given in the paper, in particular those in relation to the blasting data, reflect only those of the authors but not of the Special Duties (Works) Division and Ove Arup and Partners.

Appendix: A Template for Spreadsheet Analysis



Summary of the procedure:

1. Input the raw data, including measurements of v_m , W , and d (columns A–D).
2. Calculate the following parameters: $\ln(v_m)$, SD_2 [see Eq. (1)], $\ln(SD_2)$, $[\ln(SD_2)]^2$, and $[\ln(SD_2) \cdot \ln(v_m)]$, as required in Eq. (9). List them in columns F–J.
3. Evaluate the optimal fitting coefficients (cells M11–M18) according to Eq. (9).
4. Calculate \hat{J}_g and $\hat{\sigma}_\varepsilon^2$ according to Eqs. (8) and (10) (cells M20–M21).
5. Evaluate the covariance matrix [see Eq. (11)] (cells M25–M27).
6. Compute $\ln v(\ln \hat{a}_2, \hat{b}_2)$ for each blast based on Eq. (6) (column O).
7. Calculate ε^2 based on $\varepsilon^2 = [\ln v_m - \ln v(\ln \hat{a}_2, \hat{b}_2)]^2$ [see Eq. (6)] (column P).
8. Specify χ according to $\chi = \Phi^{-1}(0.5 + P/2)$ (see cell S10).
9. Calculate $\text{Var}(\ln v_m)$ at different SD_2 [see Eq. (15)] (column T).
10. Evaluate the upper and lower bounds of v based on Eq. (16).

References

- Ambraseys NN, Hendron AJ Jr (1968) Dynamic behaviour of rock masses. In: Stagg KG, Zienkiewicz OC (eds) *Rock mechanics in engineering practice*. Wiley, New York, pp 203–236
- Buildings Department (2004) Code of practice for foundations. Buildings Department, Hong Kong SAR Government
- Buildings Department (2007) Practice notes for authorized persons, registered structural engineers and registered geotechnical engineers. APP-72: control of blasting. Buildings Department, Hong Kong SAR Government
- Buildings Department (2009) Practice notes for authorized persons, registered structural engineers and registered geotechnical engineers. APP-24: railway protection; railways ordinance; mass transit railway (land resumption and related provisions) ordinance; area number 3 of the scheduled areas in schedule 5, buildings ordinance, cap 123. Buildings Department, Hong Kong SAR Government
- Beck JL, Katafygiotis LS (1998) Updating models and their uncertainties. I: Bayesian statistical framework. *J Eng Mech* 124(4):455–461
- Benjamin JR, Cornell CA (1970) *Probability, statistics and decision for civil engineers*. McGraw-Hill, New York
- Blair DP (2004) Charge weight scaling laws and the superposition of blast vibration waves. *Fragblast* 8(4):221–239
- Blair DP (2011a) A probabilistic analysis of vibration based on measured data and charge weight scaling. In: *Proceedings of the 6th EFEE World Conference on Explosives and Blasting Technique*, Lisbon, Portugal, September 2011, pp 319–337
- Blair DP (2011b) Making the most of blast measurements. Keynote Address, Explo 2011, Melbourne, Australia, November 2011, pp 3–10
- Bureau of Indian Standards (BIS) (1973) Criteria for safety and design of structures subjected to underground blast. ISI bulletin IS-6922
- Cao Z, Wang Y (2012) Bayesian approach for probabilistic site characterization using cone penetration tests. *J Geotech Geoenviron Eng* 139(2):267–276. doi:10.1061/(ASCE)GT.1943-5606.0000765
- Cao Z, Wang Y (2014) Bayesian model comparison and selection of spatial correlation functions for soil parameters. *Struct Saf*. doi:10.1016/j.strusafe.2013.06.003
- Ching J, Phoon K-K (2012) Modeling parameters of structured clays as a multivariate normal distribution. *Can Geotech J* 49(5):522–545
- Ching J, Phoon K-K, Chen Y-C (2010) Reducing shear strength uncertainties in clays by multivariate correlations. *Can Geotech J* 47(1):16–33
- Ching J, Chen J-R, Yeh J-Y, Phoon K-K (2012) Updating uncertainties in friction angles of clean sands. *J Geotech Geoenviron Eng* 138(2):217–229
- Chiu CF, Yan WM, Yuen K-V (2012a) Reliability analysis of soil-water characteristics curve and its application to slope stability analysis. *Eng Geol* 135–136:83–91
- Chiu CF, Yan WM, Yuen K-V (2012b) Estimation of water retention curve of granular soils from particle-size distribution—a Bayesian probabilistic approach. *Can Geotech J* 49(9):1024–1035
- Davies B, Farmer IW, Attewell PB (1964) Ground vibrations from shallow subsurface blasts. *Engineer* 217:553–559
- Dowding CH (1985) *Blast vibration monitoring and control*. Prentice-Hall, Englewood Cliffs
- Dowding CH (1996) *Construction vibrations*. Prentice-Hall, Englewood Cliffs
- Draper NR, Smith H (1981) *Applied regression analysis*, 2nd edn. Wiley, New York
- Duvall WI, Petkof B (1959) Spherical propagation of explosion generated strain pulses in rock. USBM Report of Investigation 5483
- Fenton GA, Griffiths DV (2005) Three-dimensional probabilistic foundation settlement. *J Geotech Geoenviron Eng* 131(2):232–239
- Fenton GA, Griffiths DV (2008) *Risk assessment in geotechnical engineering*. Wiley, New York
- Geotechnical Engineering Office (GEO) (2006) GEO circular no. 27. Geotechnical control of blasting. Geotechnical Engineering Office, Civil Engineering Department, Hong Kong SAR Government
- Ghosh A, Daemen JK (1983) A simple new blast vibration predictor. In: *Proceedings of the 24th US Rock Mechanics Symposium (USRMS)*, College Station, Texas, June 1983, pp 151–161
- Griffiths DV, Fenton GA (1998) Probabilistic analysis of exit gradients due to steady seepage. *J Geotech Geoenviron Eng* 124(9):789–797
- Griffiths DV, Huang J, Fenton GA (2009) Influence of spatial variability on slope reliability using 2-D random fields. *J Geotech Geoenviron Eng* 135(10):1367–1378
- Hastings WK (1970) Monte Carlo sampling methods using Markov chains and their applications. *Biometrika* 57(1):97–109
- Hong Kong Special Administrative Region (HKSAR) (2006) General specification for civil engineering works. Hong Kong SAR Government
- Huang J, Griffiths DV, Fenton GA (2010) Probabilistic analysis of coupled soil consolidation. *J Geotech Geoenviron Eng* 136(3):417–430
- Langefors U, Kihlström B (1963) *The modern technique of rock blasting*. Wiley, New York
- Li UK, Ng SY (1992) Prediction of blast vibration and current practice of measurement in Hong Kong. In: *Proceedings of the Conference Asia Pacific—Quarrying the Rim*, Hong Kong, April 1992, pp 119–135
- Metropolis N, Rosenbluth AW, Rosenbluth MN, Teller AH, Teller E (1953) Equation of state calculations by fast computing machines. *J Chem Phys* 21(6):1087–1092

- Needham J (1987) Science and civilisation in China. Volume 5: chemistry and chemical technology. Part 7: military technology: the gunpowder epic. Cambridge University Press, Cambridge
- Pal Roy P (1993) Putting ground vibration predictors into practice. *Colliery Guardian* 241:63–70
- Persson P-A, Holmberg R, Lee J (1993) Rock blasting and explosives engineering. CRC Press, Boca Raton
- Phoon K-K, Kulhawy FH (2005) Characterisation of model uncertainties for laterally loaded rigid drilled shafts. *Géotechnique* 55(1):45–54
- Phoon K-K, Santoso A, Quek S-T (2010) Probabilistic analysis of soil-water characteristic curves. *J Geotech Geoenviron Eng* 136(3):445–455
- Wang Y (2011) Reliability-based design of spread foundations by Monte Carlo simulations. *Géotechnique* 61(8):677–685
- Wang Y, Au S-K, Cao Z (2010) Bayesian approach for probabilistic characterization of sand friction angles. *Eng Geol* 114(3–4):354–363
- Wong HN, Pang PLR (1992) Assessment of stability of slopes subjected to blasting vibration. GEO report no. 15. Civil Engineering and Development Department, Hong Kong SAR Government
- Yan WM, Yuen K-V, Yoon GL (2009) Bayesian probabilistic approach for the correlations of compression index for marine clays. *J Geotech Geoenviron Eng* 135(12):1932–1940
- Yan WM, Tham LG, Yuen K-V (2012) Reliability of the design formula of blast-induced vibrations. In: Proceedings of the 13th World Conference of the Associated Research Centers for the Urban Underground Space, Singapore, November 2012, pp 1112–1118
- Yan WM, Tham LG, Yuen K-V (2013) Reliability of empirical relation on the attenuation of blast-induced vibrations. *Int J Rock Mech Min Sci* 59:160–165
- Yuen K-V (2010a) Bayesian methods for structural dynamics and civil engineering. Wiley, New York
- Yuen K-V (2010b) Recent developments of Bayesian model class selection and applications in civil engineering. *Struct Saf* 32(5):338–346
- Yuen K-V, Katafygiotis LS (2005) An efficient simulation method for reliability analysis of linear dynamical systems using simple additive rules of probability. *Probabl Eng Mech* 20(1):109–114
- Yuen K-V, Kuok S-C (2011) Bayesian methods for updating dynamic models. *Appl Mech Rev* 64(1):010802-1–010802-18
- Yuen K-V, Mu H-Q (2011) Peak ground acceleration estimation by linear and nonlinear models with reduced order Monte Carlo simulation. *Comp Aided Civ Infra Eng* 26(1):30–47
- Zhang LM, Tang WH, Zhang LL, Zheng JG (2004) Reducing uncertainty of prediction from empirical correlations. *J Geotech Geoenviron Eng* 130(5):526–534
- Zhang J, Zhang LM, Tang WH (2009) Bayesian framework for characterizing geotechnical model uncertainty. *J Geotech Geoenviron Eng* 135(7):932–940